IOSR Journal of Applied Chemistry (IOSR-JAC)
e-ISSN: 2278-5736.Volume 7, Issue 11 Ver. II. (Nov. 2014), PP 24-29
www.iosrjournals.org

Characterization of silicon-substituted hydroxyapatite powders synthesized by a wet precipitation method

A. El Yacoubi[1], A. Massit[1], M. Fathi[1], B. Chafik El Idrissi[1], K. Yamni[2]
[1]*Equipe physique des surfaces et interfaces, Laboratoire de génie physique et environnement, Faculté des Sciences B.P 133, Kénitra, Université Ibn Tofail, Maroc*
[2]*Equipe des Matériaux, Membranes et Procédés de Séparation. Faculté des Sciences Meknès, Université Moulay Ismail. Maroc*

Abstract: *The preparation of nano sized silicated hydroxyapatite $Ca_{10}(PO_4)_{6-x}(SiO_4)_x(OH)_{2-x}$ (Si-HA) with three different silicon concentrations were investigated using a wet precipitation method. The effects of the Si substitution on crystallite size, lattice parameters and fraction of crystalline phase of the powders were discussed. The crystalline phase, chemical composition,and crystallite size of hydroxyapatite and silicon substituted hydroxyapatites were characterized by X-ray diffraction (XRD), Fourier transform infrared spectroscopy (FTIR), inductively coupled plasma and transmission electron microscopy. The crystallite size and fraction of crystalline phase decreases with increase in silicon content and particle morphology spheroidal for pure hydroxyapatite changes to elongated ellipsoidalcrystals while silicon substitution increases. FTIR analysis reveals, the silicon incorporation to hydroxyapatite lattice occurs via substitution of silicate groups for phosphate groups. Substitution of phosphate group by silicate in the Si-HA structure results an increase in the lattice parameters in both a-axis and c-axis of the unit cell.*

Keywords: *Silicon-substituted hydroxyapatite, Biomaterials, FTIR, XRD.*

I. Introduction

Hydroxyapatite, [$Ca_{10}(PO4)_6(OH)_2$, HA], has a significant interest as a biomedical material for bone repair, such as bone-filling materials, biocompatible coatings for metal implant and inorganic/organic composite tissue engineering scaffolds. However, a disadvantage of using a pure HA implants is that its reactivity with existing bone is low [1] and therefore it integrates relatively slowly with bone [2]. These properties could have implications for the time required for patient rehabilitation [3]. The development of enhanced synthetic materials for use in orthopedic implants to replace lost or damaged human bone is a continual aim of bio-materials research. The bioactive behavior of HA has been improved by substituting certain ions in the apatite structure and obtain a substituted apatite which resemble the chemical composition and structure of the mineral phase in bones [4–6]. There are various substitutions that exist in the actual human bone mineral, and these include Na, Mg, K, Sr, Zn, Ba, Cu, Al, Fe, F, Cl and Si [7]. Silicon is one of the trace elements known to be essential in biological processes. Its importance on bone formation and calcification has been demonstrated through in vitro and in vivo studies [8], while the amount of silicon present within active calcification sites is related to ‘‘maturity’’ of the bone mineral. As a calcifying agent, silicon enhances the bone in growth rates of bioactive prosthetic materials, while its incorporation in the HA lattice is considered to be a potential method for improving the bioactivity of HA. Synthetic Si-HA has shown enhanced in vitro apatite formation in simulated body fluid (SBF), increased in vitro cell proliferation and creation of focal points of adhesion, as well as in vivo bone in growth and remodeling [9]. The Si-HA structure corresponds tosubstitution of phosphate ions (PO_4^{3-}) by silicate ions (SiO_4^{4-}) in the HA crystal structure. Different mechanisms for charge compensation have been suggested [10-12]. The most cited was proposed by Gibson et al. with the creation of anionic vacancies at OH^- sites [10, 13]. This mechanism leads to Si-HAs with the general formula $Ca_{10}(PO_4)_{6-x}(SiO_4)_x(OH)_{2-x}(V_{OH})_x$, where x is the molar number of silicate groups introduced into the apatitic structure ($0 \leq x \leq 2$) and V_{OH} represents vacancies maintaining the charge balance. The incorporation of Si into the HA structure in solid solution, i.e. without the formation of other phases, seems to be limited. However, the value and origin of this limitation are still not known, with, for instance, the following values being proposed: 5 wt.% [14–16], 4 wt.% [17,18], 3.1 wt.% [19], 2 wt.% [12,20], 1.0 wt.% [21] or 0.28 wt.% [22]. Si-substituted HA (Si-HA) has been synthesized using different methods such as the sol–gel route [23], solid state reactions [11], hydrothermal techniques [6, 24], microwave irradiation [25] and precipitation from aqueous solutions [10, 26, 27]. Each having its own advantages and disadvantages, aqueous precipitation methods are the most often described in the literature, it is the most talented route owing to its ease in experiment operations, low working temperature, high percentages of pure products and inexpensive equipment requirement [28,29].

The aim of this research is to synthesize approximately pure Si-substituted hydroxyapatite with controlled silicate amount by aqueous precipitation method and investigate the effect of Si content on the grain

size.The effect of Si substitution on the different functional groups, such as hydroxyl (OH^-), phosphate (PO_4^{3-}) and silicate (SiO_4^{4-}) groups of Si-HA was also been investigated.

II. Materials and methods:

2.1. Materials:

A pure HA $Ca_{10}(PO_4)_6(OH)_2$ was first prepared to be used as a reference material for further Si-HA syntheses and analyses. This was prepared following the aqueous precipitation method described in Ref. [30]. Si-HA powders were prepared through an aqueous precipitation method based on the chemical formula $Ca_{10}(PO_4)_{6-x}(SiO_4)_x(OH)_{2-x}$ proposed by Gibson et al [10]. The amount of reagents was calculated according to the assumption that one silicate ion would substitute for one phosphate ion using calcium hydroxide ($Ca(OH)_2$), phosphoric acid (H_3PO_4) and tetraethoxysilane ($Si(OCH_2CH_3)_4$) (TEOS) solutions as reagents, the amount of reagents is listed in Table 1. Three grades of silicate-substituted HA (Si-HA) powders were synthesized by maintaining the Ca/(P+Si) ratios fixed at 1.67 and Ca/P is in the range 2.17 to 2.40 as represented in Table 1.

An aqueous solution of H_3PO_4 and $Si(OCH_2CH_3)_4$ was added drop by drop (150 µl/s) into $Ca(OH)_2$ under-stirring aqueous suspension. The pH of reaction mixture remained greater than 10 without addition of ammonia solution. After total addition of the H_3PO_4 and $Si(OCH_2CH_3)_4$ solution, the reaction mixture was stirred for 2h at the same medium temperature and then matured over a period of 48 h at ambient temperature.

These matured suspensions were decanted and subjected to thermal treatment at 90°C for 24 h and subsequently ground to a fine powder in an agate mortar. The resulting oven-dried precipitates were calcined at 900°C in a dry air atmosphere using a ramp of 5°C/min with a soaking time of 1 h at peak temperature, and then cooled in a furnace to ambient temperature at a cooling rate of 10°C/min.

2.2. Characterization:

The crystalline phases of powders were determined using X-ray diffraction (XRD) they were identified by means of a XPERT-PROPW3050/60 (Theta/Theta) using CuKα radiation and operating at 45 kV and 40 mA and counting time of 0.5°/mn. Crystalline phases detected in the patterns were identified by comparison to standard patterns from the ICDD-PDF (International Center for Diffraction Data-Powder Diffraction Files). The values of full width at half-maximum (FWHM) of the peak of the (002) plane, representative of the crystallites along the c-axis, and of the peak ofthe (300) plane, representative of the crystallites along the a-axis,were used in the calculation according to the Scherrer's [31] equation (1):

$$D = k \lambda / \beta \cos\theta \quad (1)$$

where D is the crystallite size in Å, k is Scherrer constant (0.89), λ is the wavelength of X-rays beam (1.5406 Å), θ is the diffraction angle and β is defined as the diffraction FWHW, expressed in radians. Determination of the lattice constants of HA and Si-HA was made by refinement of XRD data of samples calcined at 900°Cusing Fullprof-suite software program.

The fraction of crystalline phase (Xc) of the HA and Si-HA powders was evaluated by the following equation, equation (2) [32]:

$$X_C = 1 - \nu_{112/300}/I_{300} \quad (2)$$

Where I_{300} is the intensity of (3 0 0) diffraction peak and $\nu_{112/300}$ is the intensity of the hollow between (112) and (3 0 0) diffraction peaks of HA.

Fourier transformed IR (FTIR) absorption spectra of powders were obtained using a Vortex 70 spectrometerin order to analyze the functional groups. One percent (1%) of the powder was mixed and ground with 99% KBr. Tablets of 10 mm diameter for FTIR measurements were prepared by pressing the powder mixture at a load of 5 tons for 2 min and the spectrum was taken in the range of 400 to 4000 cm^{-1} with resolution 4 and 128 times scanning.

TECNAI G2/FEI Transmission electron microscopy (TEM), operating at an accelerating voltage of 200 kV, was employed for characterization of the microstructure of HA and Si-HA.

The Ca/P ratio of the calcined powder was measured by inductively coupled plasma ICP-AES atomic emission spectroscopy (modela2- JobinYvon).

III. Results and discussion

Chemical analyses of the obtained precipitations as determined by ICP are summarized in Table 1.The phosphorus content is lower than that of the corresponding amount of starting material because the presence of CO_2 in solution during the synthesis carbonate groups can replace some phosphorus sites and hence carbonated apatite was formed; as evidenced by FTIR technic.

Table 1: Quantities of reactants (mol) and expected molar ratios for the samples

Sample	$Ca(OH)_2$	H_3PO_4	TEOS	Si (wt.%)	x	Ca/P	Ca/P [(a)]	Chemical formula of Si_xHA
HA	0.0200	0.0100	-	-	-	1.67	1.66	$Ca_{10}(PO_4)_6(OH)_2$
$Si_{1.4}HA$	0.0200	0.0092	0.0028	3.9	1.4	2.17	1.91	$Ca_{10}(PO_4)_{4.6}(SiO_4)_{1.4}(OH)_{0.6}$
$Si_{1.6}HA$	0.0200	0.0088	0.0032	4.4	1.6	2.27	2.17	$Ca_{10}(PO_4)_{4.4}(SiO_4)_{1.6}(OH)_{0.4}$
$Si_{1.6}HA$	0.0200	0.0083	0.0037	5.1	1.8	2.40	2.35	$Ca_{10}(PO_4)_{4.2}(SiO_4)_{1.8}(OH)_{0.2}$

[(a)]Determined by ICP/AES.

The X-ray diffraction patterns of powders are shown in Fig. 1. The X-ray diffraction patterns of samples calcined at 900 °C for 1 h indicate that the diffraction peaks can be indexed based on JCPDS Card No. 09-0432 and do not reveal the presence of any phases related to a silicon oxide or other calcium phosphate species.

In a first order approximation silicon substitution does not affect the diffraction pattern of hydroxyapatite. Although the XRD patterns virtually correspond to that of pure HA, the diffraction peaks lose intensity with increasing Silicate content. Also the broadening of the X-ray peaks indicates the decrease of crystallinity and crystallite size.

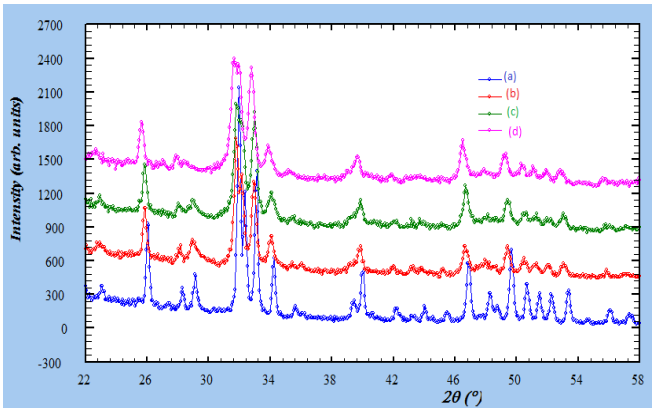

Fig. 1.X-ray powder diffraction patterns of HA and Si-HA powders calcined at 900°C

The lattice parameters of pure, Si-substituted hydroxyapatite samples and the unit cell volume are listed in table 2. It can be seen that the unit cell parameters and unit cell volume of Si-HA are larger than that of pure HA. The increase in the lattice parameters of Si-HA result from a slight shift of the Si-HA peaks to a lower Bragg's angle compared to a pure HA, as shown in Fig. 2.

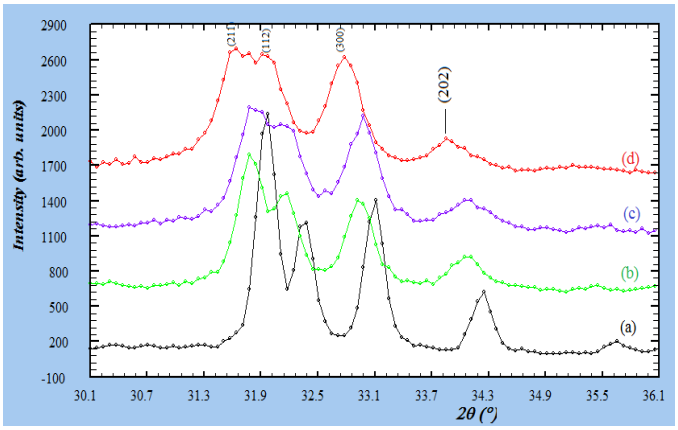

Fig. 2. Peak shift for Si-HA samples with increasing silicon content (a) pure HA, (b) $Si_{1.4}HA$, (c) $Si_{1.6}HA$ and (d) $Si_{1.8}HA$.

The larger lattice parameters of Si-substituted HA relative to those of stoichiometric HA can be understood considering that the average lengths of the Si-O and P-O bonds are 1.62 and 1.51 Å, respectively. Therefore, the substitution of PO_4^{3-} by SiO_4^{4-} is assumed to contribute to the increase in the lattice parameters of the Si-HA materials. Both a and c parameters increase as the level of Si substitution increases. These changes also appear logical considering that the ionic radius of Si^{4+} (0.042 nm) is larger than that of P^{5+} (0.035 nm). However, the observed variations in the lattice parameters and crystallite sizes did not change the intensity of the XRD peaks. This can also be understood considering that apparent intensity changes in the XRD peaks are

only expected when there is an extensive atomic substitution of fairly different sized ions. In the present case, Si and P are adjacent to each other in the periodic table differing only by one atomic number and the Si levels are relatively low. This could be attributed to different charge compensation mechanism for isomorphous substitution of PO_4^{3-} by SiO_4^{4-}.

Table 2: Lattice parameters and unit cell volume of HA and Si-HA calcined at 900°C

Sample	a (Å)	c (Å)	V(Å^3)
HA	9.4142	6.8802	528
Si1.4HA	9.4224	6.9070	531
Si1.6HA	9.4352	6.9078	532
Si1.8HA	9.4388	6.9132	533

The crystallite sizes, determined by using Scherrer's equation along a and c crystallographic axis, are given in Table 3. Increasing the Si content from 3.9 to 5.1 wt. %, the crystallite size decreases from 40 nm to 25 nm along a axis and 31 nm to 25 nm along c axis. The pure HA shows 41 nm and 42 nm along a and c axis respectively. This indicates that; increase in silicon substitution affects the size and the morphology of the crystallites present in the powder; spheroidal to high aspect ratio ellipsoidal shape crystallites with increase in Si substitution.

Table 3: Crystallite sizes along a-axis and c-axis of calcined HA and Si-HA using Scherrer's equation and degree of crystallinity (%)

Sample	Crystallite size along a-axis (Å)	Crystallite size along c-axis (Å)	degree of crystallinity (%)
HA	41	42	82
Si1.4HA	40	31	66
Si1.6HA	40	29	61
Si1.8HA	32	25	57

FTIR was used to study the effect of the silicon substitution on the different functional groups, such as hydroxyl and phosphate groups of hydroxyapatite. The figure 3 shows the FTIR spectra of powders calcined at 900°C for 1 h. The intense bands at 1100, 1034, and 962 cm^{-1}correspond to P-O stretching vibration modes, whereas the doublet at 603-567 cm^{-1} corresponds to the O-P-O bending mode. The bands at 3572 and 631cm^{-1} correspond to the stretching and bending modes, respectively, of the hydroxyl groups in hexagonal channels. The infrared symmetric and asymmetric P-O stretching bands decrease and become less resolved as the silicate contents increase, as shown in Fig. 3. Similar changes are also observed in the doublet at 603-565 cm^{-1}, corresponding to the asymmetric bending motion of phosphate groups. However, the positions of both stretching and bending bands are obviously unaffected by the silicate substitution. The most notable effect of silicate substitution in HA is the change in the hydroxyl stretching and the bending bands at 3572 and 631 cm^{-1}, respectively. The Figure 3 shows that the intensities of the bands at 3572 and 631 cm^{-1} of silicate substituted samples decrease with the increasing silicate substitution level and both bands nearly disappear for sample $Si_{1.8}HA$, which could be attributed by the charge compensation mechanism in which HA unit cell loses one OH^- group for the substitution of the phosphate group by silicate group. Bands in the region associated with the CO_3^{2-} vibration mode (1550–1410 cm^{-1}) were also present. The present absorption spectra, which are in close agreement with previous studies [13,18] indicate that CO_3^{2-} groups have substituted both PO_4^{3-} and OH^- groups in the HA structure. Additional three low intensity bands appear at approximately 490, 756 and 890 cm^{-1}, which do not appear in reference HA samples. These three peaks have been attributed to the presence of SiO_4^{4-} groups in the Si-HA structure [11, 33]. Incorporation of silicon into hydroxyapatite ($Ca_{10}(PO_4)_{6-x}(SiO_4)_x(OH)_{2-x}$) also changes hydroxyl stretching bands at 630 and 3570 cm^{-1}. The substitution of PO_4^{3-} by SiO_4^{4-} reduces the amount of hydroxyl groups required for charge balance. Moreover, as the Si content is increased, there is a strong intensity loss of the CO_3^{2-} related absorption bands [12, 33]. This result also supports the idea that SiO_4^{4-} substitute PO_4^{3-} tetrahedra in the hydroxyapatite structure since CO_3^{2-} groups occupy both PO_4^{3-} and OH^- sites.

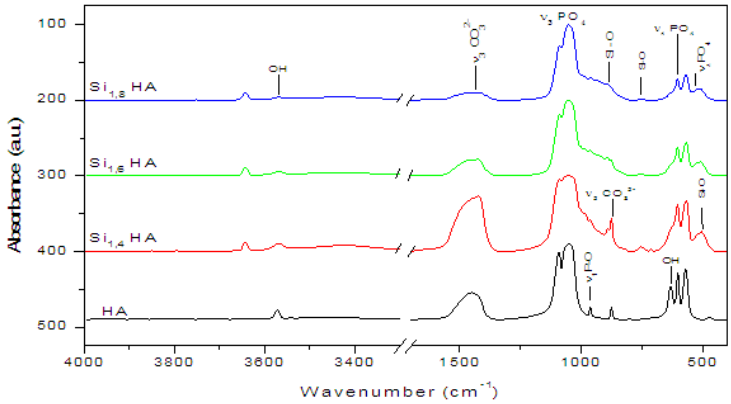

Fig.3. FTIR spectra of HA and Si-HA powders.

TEM micrographs of the HA and Si-HA powders calcined at 900°C are given in Fig. 4. The Si content has a negative effect on the crystal size, the mean value of crystal size decreases with the increase of Si content. The figue 4 shows that the pure HA is spheroidal-shaped crystallites, however, increase with the Si content, the crystals started elongating and $Si_{1.8}$HA powder shows ellipsoidal shape morphology, suggesting that the growth perpendicular to the c-axis is easier in the presence of Si.

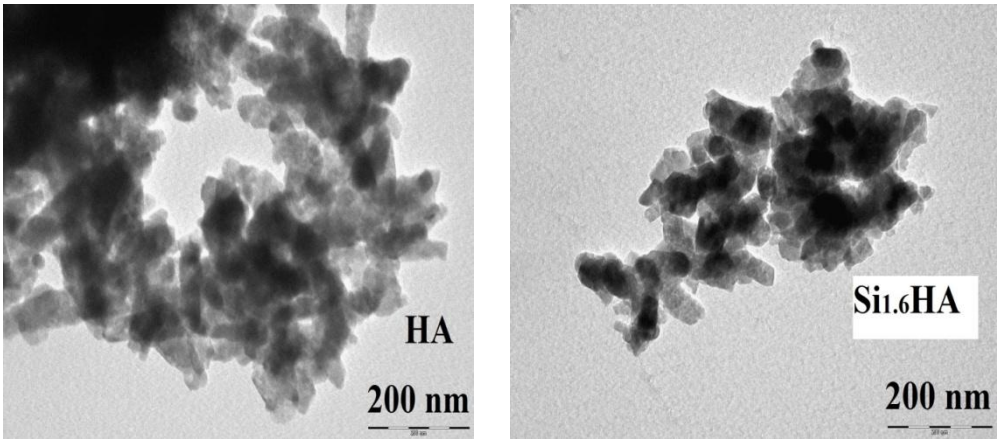

Fig. 4. TEM Micrographs of HA and $Si_{1.6}$HA powders calcined at 900°C

IV. Conclusion

Silicon-substituted hydroxyapatite powders were prepared by a wet precipitation method using $Ca(OH)_2$, H_3PO_4 and $Si(OCH_2CH_3)_4$ (TEOS) solutions as reagents. The analysis of XRD, FTIR and TEM shows that the substitution of the silicate groups for the phosphate groups causes some OH^- loss to maintain the charge balance and changes the lattice parameters and the unit cell volume of HA. Furthermore, TEM and XRD results show that incorporation of silicate groups reduces Si-HA fraction of crystalline phase and crystallite size.

References

[1]. P. Ducheyne, S. Radin, L. King, The effect of calcium-phosphate ceramic composition and structure on in vitro behaviour. I. Dissolution, J. Biomed. Mater.27 (1993) 25e34.
[2]. E. Schepers, M. Declercq, P. Ducheyne, R. Kempeneers, Bioactive glass particulate material as a filler for bone lesions, J. Oral Rehab.18 (1991) 439e452.
[3]. A.E. Porter, N. Patel, J.N. Skepper, S.M. Best, W. Bonfield, Effect of sintered silicate-substituted hydroxyapatite on remodeling processes at the bone-implant interface, Biomaterials 25 (2004) 3303e3314.
[4]. V.R. Maria, A. Daniel, Silicon substituted hydroxyapatite. A method to upgrade calcium phosphate based implants,J. Mater. Chem. 15 (2005) 1509–1516.
[5]. F. Balas, J.P. Pariente, M.V. Regi, In vitro bioactivity of silicon-substituted hydroxyapatites, J. Biomed.Mater. Res. 66A (2003) 364–375.
[6]. A. Aminian, M. Hashjin, A. Samadikuchaksaraei, F. Bakhshi, F.Gorji- pour, A. Farzadi, F. Moztarzadeh, M.Schmcker, Synthesis of silicon-substituted hydroxyapatite by a hydrothermal method with two different phosphorous sources, Ceram. Int. 37 (2011) 1219–2122.
[7]. A.M. Pietak, J.W. Reid, M.J. Stott, M. Sayer, Silicon substitution in thecalcium phosphate bioceramics, Biomaterials 28 (2007) 4023–4032.
[8]. Carlisle EM. Silicon: a possible factor in bone calcification. Science 1969;167:279–80.

[9]. A.E. Porter, N. Patel, J.N. Skepper, S.M. Best, W. Bonfield, Effect of sintered silicate-substituted hydroxyapatite on remodeling processes at the bone-implant interface, Biomaterials 25 (2004) 3303e3314.

[10]. Gibson IR, Best SM, Bonfield W. Chemical characterization of silicon-substituted hydroxyapatite. J Biomed Mater Res 1999;44:422–8.

[11]. Arcos D, Rodríguez-Carvajal J, Vallet-Regí M. The effect of silicon incorporation on the hydroxylapatite structure.A neutron diffraction study. Solid State Sci 2004;6:987–94.

[12]. Astala R, Calderin L, Yin X, Stott MJ. Ab initio simulation of Si-doped hydroxyapatite.Chem Mater 2006;18:413–22.

[13]. Gibson IR, Huang J, Best SM, Bonfield W. Enhanced in vitro cell activity and surface apatite layer formation on novel silicon-substituted hydroxyapatites. Bioceramics 1999; 12:191–4.

[14]. Best S, BonfieldW, Gi R, Jha LJ, Da Silva Santos JD. Silicon-substituted apatites and process for the preparation thereof.US patent US 6,312,468 B1; 1998.

[15]. Thian ES, Huang J, Vickers ME, Best SM, Barber ZH, Bonfield W. Silicon- substituted hydroxyapatite (SiHA): a novel calcium phosphate coating for biomedical applications. J Mater Sci 2006;41:709–17.

[16]. Vallet-Regí M, Arcos D. Silicon substituted hydroxyapatites. A method to upgrade calcium phosphate based implants. J Mater Chem 2005;15.

[17]. Gasquères G, Bonhomme C, Maquet J, Babonneau F, Hayakawa S, Kanaya T et al. Revisiting silicate substituted hydroxyapatite by solid-state NMR. MagnResonChem 2008;46:342–6.

[18]. Tang XL, Xiao XF, Liu RF. Structural characterization of silicon-substituted hydroxyapatite synthesized by a hydrothermal method. Mater Lett 2005;59:3841–6.

[19]. Gomes S, Nedelec J-M, Jallot E, Sheptyakov D, Renaudin G. Silicon location in silicate-substituted caclium phosphate ceramics determined by neutron diffraction. Cryst Growth Des 2011;11:4017–26.

[20]. Kim SR, Lee JH, Kim YT, Riu DH, Jung SJ, Lee YJ, et al. Synthesis of Si, Mg substituted hydroxyapatites and their sintering behaviors. Biomaterials 2003;24:1389–98.

[21]. Ruys AJ. Silicon-doped hydroxyapatite. J Aust Ceram Soc 1993;29:71–80.

[22]. Putlayev V, Veresov A, Pulkin M, Soin A, Kuznetsov V. Silicon-substituted hydroxyapatite ceramics (Si-HAP): densification and grain growth through the prism of sintering theories. Mater SciEngTechnol 2006;37:416–21.

[23]. Hijón N, Victoria Cabañas M, Peña J, Vallet-Regí M. Dip coated silicon-substituted hydroxyapatite films. ActaBiomater 2006;2:567–74.

[24]. Kim YH, Song H, Riu DH, Kim SR, Kim HJ, Moon JH. Preparation of porous Si-incorporated hydroxyapatite.CurrApplPhys 2005;5:538–41.

[25]. Sanosh Kunjalukkal Padmanabhan, EhsanUlHaq, Antonio Licciulli. Rapid synthesis and characterization of silicon substituted nano-hydroxyapatite using microwave irradiation. Current Applied Physics 14 (2014) 87-92.

[26]. Bianco A, Cacciotti I, Lombardi M,Montanaro L. Si-substituted hydroxyapatite nanopowders: synthesis, thermal stability and sinterability. Mater Res Bull 2009;44:345–54.

[27]. Palard M, Champion E, Foucaud S. Synthesis of silicated hydroxyapatite $Ca_{10}(PO_4)_{6-x}(SiO_4)_x(OH)_{2-x}$. J Solid State Chem 2008;181:1950–60.

[28]. Cao, L., Zhang, C. and Huang, J. 2005. Synthesis of hydroxyapatite nanoparticles in ultrasonic precipitation.Ceram. Int. 31 : 1041-1044.

[29]. Kong, L.B., Ma, J. and Boey, F. 2002. Nano- sized hydroxyapatite powders derived from coprecipitation process. J. Mater. Sci. 37 : 1131-1134.

[30]. B. Chafik El Idrissi, K. Yamni, A. Yacoubi, A. Massit, A novel method to synthesize nanocrystalline hydroxyapatite: Characterization with x-ray diffraction and infrared spectroscopy,IOSR Journal of Applied ChemistryVolume 7, Issue 5 Ver. III. (May. 2014), PP 107-112.

[31]. L.A. Azaroff, Elements of X-ray Crystallography, McGraw-Hill, New York, 1968. pp. 38–42

[32]. B.S. HaiboWang, Hydroxyapatite degradation and biocompatibility, dissertation, The Ohio State University, 2004.

[33]. Alieh Aminian, Mehran Solati-Hashjin, Ali Samadikuchaksaraei, Farhad Bakhshi, Fazel Gorjipour, Arghavan Farzadi, Fattolah Moztarzadeh, Martin Schmucker, Synthesis of silicon-substituted hydroxyapatite by a hydrothermal method with two different phosphorous sources,Ceramics International 37 (2011) 1219–1229

[34]. E.L. Solla, F.Malz, P. Gonza ´lez, J. Serra, C. Jaeger, B. Leo ´n, The role of Si-substitution into hydroxyapatite coatings, J. Key Eng. Mater. 361–363 (2008) 175–178.